Changes in the Climatology, Structure, and Seasonality of Northeast Pacific Atmospheric Rivers in CMIP5 Climate Simulations

MICHAEL D. WARNER AND CLIFFORD F. MASS

Department of Atmospheric Sciences, University of Washington, Seattle, Washington

(Manuscript received 18 August 2016, in final form 29 April 2017)

ABSTRACT

This paper describes changes in the climatology, structure, and seasonality of cool-season atmospheric rivers influencing the U.S. West Coast by examining the climate simulations from phase 5 of the Coupled Model Intercomparison Project (CMIP5) that are forced by the representative concentration pathway (RCP) 8.5 scenario. There are only slight changes in atmospheric river (AR) frequency and seasonality between historical (1970–99) and future (2070–99) periods considering the most extreme days (99th percentile) in integrated water vapor transport (IVT) along the U.S. West Coast. Changes in the 99th percentile of precipitation are only significant over the southern portion of the coast. In contrast, using the number of future days exceeding the historical 99th percentile IVT threshold produces statistically significant increases in the frequency of extreme IVT events for all winter months. The peak in future AR days appears to occur approximately one month earlier. The 10-model mean historical and end-of-century composites of extreme IVT days reflect canonical AR conditions, with a plume of high IVT extending from the coast to the southwest. The similar structure and evolution associated with ARs in the historical and future periods suggest little change in large-scale structure of such events during the upcoming century. Increases in extreme IVT intensity are primarily associated with integrated water vapor increases accompanying a warming climate. Along the southern portion of the U.S. West Coast there is less model agreement regarding the structure and intensity of ARs than along the northern portions of the coast.

1. Introduction

Narrow regions of large water vapor transport that extend from the tropics or subtropics into the extratropics, often called atmospheric rivers (ARs), are responsible for the majority of cool-season heavy precipitation events along the North American west coast (Ralph et al. 2005, 2006; Dettinger 2011; Warner et al. 2012) and are an important part of the hydrologic cycle in many locations throughout the world (e.g., Dettinger 2004; Viale and Nuñez 2011; Ralph et al. 2013; Sodemann and Stohl 2013; Lavers et al. 2013). Atmospheric rivers are often associated with flooding or landslides, with the largest events causing millions of dollars of infrastructure damage (Mastin et al. 2010; Neiman et al. 2011).

Several studies over the last few decades have examined the impacts of atmospheric rivers on coastal precipitation (e.g., Lackmann and Gyakum 1999) and described the annual climatology of such events (Neiman et al. 2008b; Warner et al. 2012; Rutz et al. 2014). Warner et al. (2012), using precipitation observations at six Pacific Northwest coastal stations over a 60-yr period (1950–2009), found that the highest frequency of AR events occurred in January, with November and December experiencing slightly fewer events. Neiman et al. (2008b) found that north of the California–Oregon border, the highest frequency of events was in October, with November a close second. South of that border, the frequency was highest in November, followed by January. In all of these studies, the synoptic structures accompanying AR events were characterized by a deep upper-level trough extending into the subtropical northeast Pacific, a ridge over the North American west coast, high values of integrated water vapor (IWV) extending northeast from the subtropics toward the coast, and exceptionally warm temperatures in the lower troposphere. A recent study (Ryoo et al. 2015) documented the trajectories associated with West Coast atmospheric rivers, showing that most are associated with ascending trajectories originating in the tropics/subtropics or the midlatitudes.

Corresponding author: Michael Warner, mdwarner@atmos.washington.edu

DOI: 10.1175/JHM-D-16-0200.1

There have been a number of studies regarding the location and intensity of atmospheric rivers under global warming. Atmospheric rivers are generally found on the warm side of midlatitude baroclinic zones (e.g., Browning and Pardoe 1973; Cordeira et al. 2013). Some studies suggest that global warming may cause such baroclinic zones and associated jet streams to weaken and move northward as the Hadley cell expands (e.g., Lu et al. 2007; Meehl et al. 2007; Chang et al. 2012; Singh and O'Gorman 2012; Barnes and Polvani 2013), although such changes would not be uniform around the globe. ARs might be expected to move northward with the midlatitude jet; however, other studies have found an equatorward shift in AR landfall associated with changes in the subtropical jet stream (Payne and Magnusdottir 2015; Shields and Kiehl 2016a). Either way, any changes in the jet stream have the potential to affect the distribution of precipitation along the North American west coast (Salathé 2006; Mass et al. 2011; Dettinger 2011; Warner et al. 2015; Shields and Kiehl 2016a). Furthermore, it is expected that increasing moisture in a warming atmosphere would increase the intensity of ARs (Dettinger 2011; Lavers et al. 2013; Salathé et al. 2014; Warner et al. 2015; Lavers et al. 2015; Gao et al. 2015).

Recently, several studies have focused on the response of AR characteristics to warming in phase 5 of the Coupled Model Intercomparison Project (CMIP5) representative concentration pathway (RCP) 8.5 projections. Gao et al. (2015) determined the change of frequency of atmospheric rivers along the west coast of North America between 1975–2004 and 2070–99 in a 24-model ensemble. Requiring that an atmospheric river had an integrated water vapor transport (IVT) moisture plume of at least 2000 km in length, they found that the number of AR days increases by 50 to 600%, depending on location. Furthermore, they noted that the declining winds along much of the west coast were compensated by substantial increases in water vapor content associated with warming. Payne and Magnusdottir (2015), examining changes in atmospheric rivers over the west coast of North America using 28 CMIP5 models, found an increase of AR frequency south of locations of peak historical frequency as a result of increasing winds and a broadening frequency distribution along the coast. They noted that areas of historical peak AR frequency had increases in magnitude due to enhancements of moisture values. Shields and Kiehl (2016a) found similar spatial changes to Payne and Magnusdottir (2015), but considered only a single relatively high-resolution climate model, CCSM4. Using this same climate model, Shields and Kiehl (2016b) determined that Pineapple Express events, high IVT events originating from the deep tropics and impacting the U.S. West Coast, are increasing in duration and intensity. Hagos et al. (2016) analyzed the change in frequency and intensity of AR events over western North America using a CMIP5-driven Community Earth System Model Large Ensemble (CESM-LE). Between the last 20 years of the twentieth and twenty-first centuries, they found a 35% increase in the number of landfalling AR days and an enhancement of 28% in extreme precipitation days.

The work described in this paper extends and expands upon the research described above. First, this paper presents information about the changes of frequency and intensities of atmospheric rivers using a different, but complementary, definition of atmospheric rivers. Second, using this definition, this work examines the changes in AR seasonality as defined by IVT at coastal locations. Third, the research described below identifies changes in the structure and spatial variability of AR moisture anomalies as the planet warms.

2. Data and methods

In this work, ARs are diagnosed using relatively low-resolution GCMs by identifying periods with the highest (99th percentile) IVT over coastal water in daily model output. This criterion is different than, but complementary to, approaches applied in many other studies (e.g., Rutz et al. 2014; Gao et al. 2015; Hagos et al. 2016), which explicitly require the existence of moisture plumes of specific length, magnitude, or width. The approach used in this study only requires large values of IVT reaching the coast,[1] the critical requirement for producing large amounts of precipitation (i.e., Neiman et al. 2002; Ralph et al. 2006; Neiman et al. 2008a; Viale and Nuñez 2011). However, evaluation of days fulfilling the criterion used in this study reveal that all are associated with plumes of moisture consistent with "classic" definitions of atmospheric rivers. To illustrate this fact, Fig. 1 shows daily mean IVT for the National Centers for Environmental Prediction–National Center for Atmospheric Research (NCEP–NCAR) reanalyses and three CMIP5 GCMs for several days, with ARs achieving the 99th percentile historical (1970–99) IVT at several points along the U.S. West Coast. All display a narrow plume of high IVT that extends thousands of kilometers toward the west or southwest into the tropical or subtropical Pacific Ocean.

Following Warner et al. (2015), this study uses daily specific humidity and zonal u and meridional v components of wind from 10 CMIP5 models to construct

[1] IVT represents the total advection of water vapor from the surface to 500 hPa.

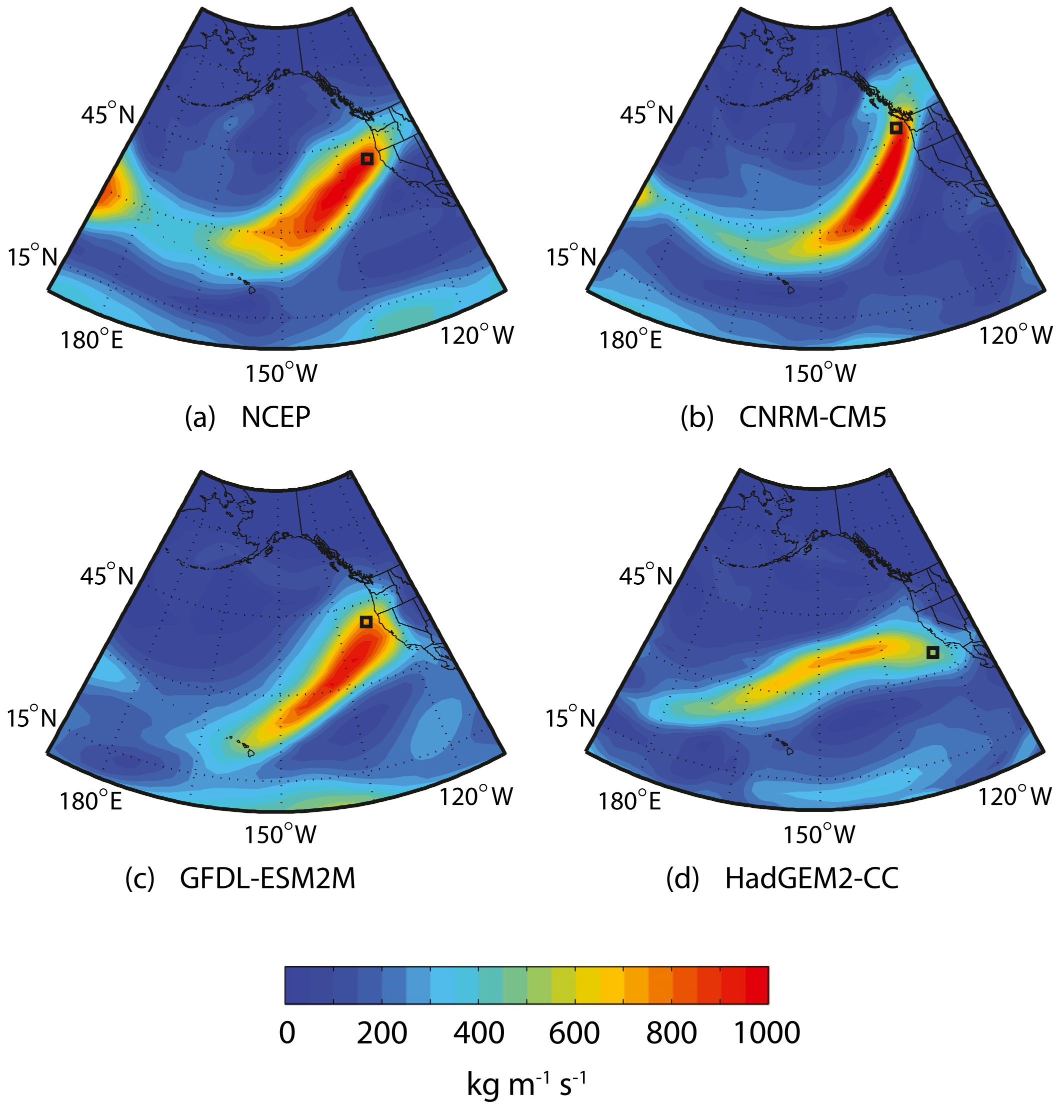

FIG. 1. Individual AR days in several models as defined by 99th percentile IVT at the indicated locations (box) offshore. (a) NCEP–NCAR reanalyses, 25 Dec 1980; (b) CNRM-CM5, 6 Dec 1975; (c) GFDL-ESM2M, 13 Jan 1980; and (d) HadGEM2-CC, 6 Dec 1990.

IVT and IWV fields for both a historical (1970–99) and a future (2070–99) period. ARs were identified by selecting the 99th percentile days in IVT at each point along a line of points offshore of the west coast of North America (Fig. 2). Each of these points was sufficiently offshore so that they were over water for all the GCMs considered (precipitation was not affected by orographic processes). Only CMIP5 climate models containing the necessary variables and with sufficient horizontal resolution to avoid land-fraction contamination were used.[2] AR days in the future period were determined in two ways: 1) days in which the IVT exceeded the 99th percentile during the future period (useful for examining intensity increases) and 2) days exceeding the 99th percentile IVT days from the historical period (useful from an infrastructure perspective). Using only the 99th percentile events produces an equal number of events in both periods.[3] In contrast, applying the historical IVT threshold in the future period

[2] More information regarding model selection processes for this study can be found in Warner et al. (2015).

[3] The mean number of days above threshold for the historical period is 55. See Warner et al. (2015, their Table 2) for more detailed information on future increases in days above the historical threshold.

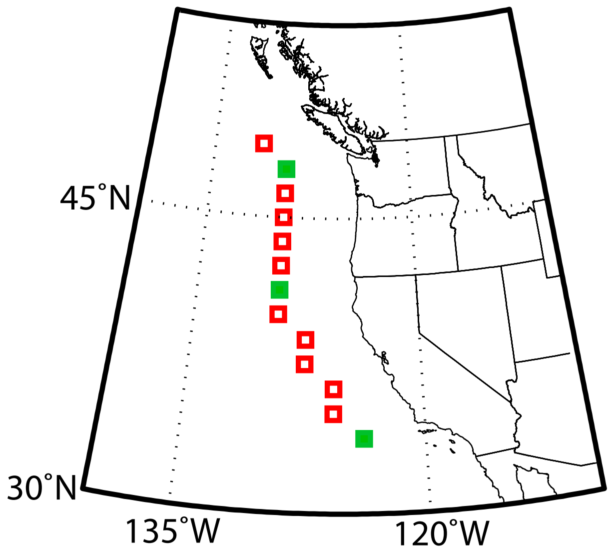

FIG. 2. Locations evaluated in CMIP5 models and reanalysis grids. Solid green boxes indicate locations highlighted in the text and other figures.

results in a large increase in the number of days above the threshold.

Once AR days were identified for each model and at each point along the transect, a seasonal climatology was constructed, providing the monthly frequency of AR days during the cool season (October–March). At each point, historical-period CMIP5 model frequencies, the NCEP–NCAR reanalyses (Kalnay et al. 1996) frequencies, and the future model frequencies for AR days were compared. Statistically significant changes at 95% were determined using the Student's t test. In addition to monthly climatologies for IVT and wind, spatial composites of IVT were created for the historical and future periods, using both 99th percentile and historical thresholds.

3. Results

a. AR seasonality

Atmospheric river climatologies were determined at each point along a coastal transect (Fig. 2). Because AR climatology varies smoothly along the West Coast, only three offshore points (indicated by green boxes) are presented here: 33.75°, 41.25°, and 47.5°N, located along the coast of Southern California, near the California–Oregon border, and offshore of northern Washington State.

Figure 3 shows the multimodel cool-season climatology of 99th percentile IVT AR days for the south, middle, and north points for both historical (blue) and future (red) periods. The black solid lines show the observed frequency derived from the NCEP–NCAR reanalyses, while the box-and-whisker plots display the ensemble of model values. The Student's t statistic is used to determine if future means are statistically different from historical means with 95% confidence (indicated by green stars).

First, consider the historical period. To the south, the reanalysis-based peak frequency is in midwinter, while to the north the highest frequency is in late autumn. The historical median model AR frequency at the south point peaks in February, followed by January, in contrast to the NCEP–NCAR reanalyses, which peak in January.[4] At the middle location near the California–Oregon border, the model historical-period median frequency peaks in January, while the NCEP–NCAR reanalyses peak a month earlier in December. The model climatology for the northern Washington coast has peak median AR frequency in December, with nearly equal frequency in October and November. In contrast, the NCEP–NCAR reanalyses peak in November and exhibit a secondary maximum in January. This secondary maximum in January was also noted in Neiman et al. (2008b) for their north coast area (41°–52.5°N, 1998–2005).

The future median AR day frequency based on the ensemble of RCP 8.5 GCM projections at the three locations is also shown in Fig. 3 (red). At the south point, the projected model median AR frequency peak is in January, one month earlier than simulated by the model during the historical period. January has the largest increase of median frequency of any month. In the middle of the domain, the models' median future projection peaks (and has the largest increases) in December, also one month earlier than in the historical period. The north point shows little change in the monthly median frequency of AR days between future and historical periods. On the whole, future projections suggest an advance of the seasonal AR maximum for the southern and middle coast locations by roughly one month by the end of the century. However, the changes are generally quite modest: for the three locations, only the medians at the south point for January and March reflect statistically significant (95% confidence level) changes between historical and future periods.

End-of-century increases in IWV lead to very large enhancements in the frequency of IVT days exceeding

[4] Similar reanalysis behavior has been observed by Mundhenk et al. (2016) in relation to AR identification along the U.S. West Coast using the NASA Modern-Era Retrospective Analysis for Research and Applications (MERRA), although that study uses 3-month periods for frequency analysis and averages over the whole West Coast.

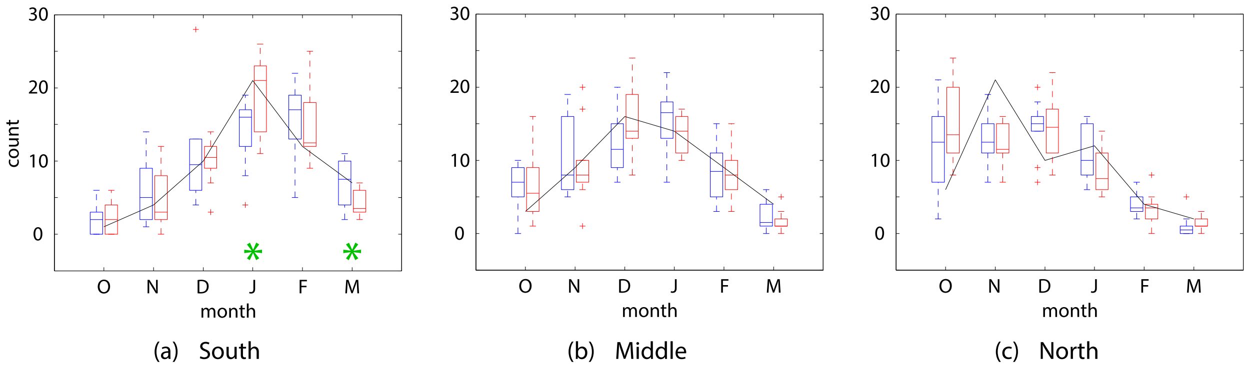

FIG. 3. Box-and-whisker plots of 10-model winter mean (October–March) climatology of AR days defined by 99th percentile IVT offshore at (a) 33.75°, (b) 41.25°, and (c) 47.5°N for the historical (1970–99, blue) and future periods (2070–99, red). The plots show the median (horizontal lines), the 75th and 25th percentiles (upper and lower range of the box, respectively), the model extremes (whiskers), and outliers from the interquartile range (plus signs). NCEP–NCAR reanalyses events are represented by black solid lines. Green asterisks indicate months with statistically significant changes in the mean with 95% confidence.

historical 99th percentile IVT threshold values (Warner et al. 2015). From an impacts perspective, this is the methodology that is most relevant, since one would expect IVT of a certain level to have the same hydrometeorological effects in the future as it does in the historical period. Figure 4 shows the climatology for AR days exceeding the historical (1970–99) threshold for both historical and future periods based on the CMIP5 10-model ensemble used in this study. The historical model results and NCEP–NCAR reanalyses are the same as in Fig. 3. In contrast to Fig. 3, Fig. 4 shows end-of-century projections that exhibit large increases in frequency above the historical 99th percentile threshold. For example, during January at the south point, there is an increase from 15 to 20 events during the historical period to around 50 events by the end of the century. Importantly, and largely due to the relationship between temperature and atmospheric water vapor content as dictated by the Clausius–Clapeyron relationship, for months with the most AR days, the median future frequency and model spread lie outside of the historical model variability, with the differences being statistically significant at the 95% level for all months and locations. Regarding timing, in the southern portion of the domain the largest increase in AR frequency is in January and February. As for the previous 99th percentile analysis, there appears to be an advance of roughly one month in the peak values. In the middle of the domain, the largest increase in frequency is in December and January, again with an apparent one-month advance. Finally, to the north, very large increases occur in October–December, suggesting a large increase in frequency of extreme events during autumn. The increases in frequency are primarily from increases in water vapor due to a warming climate, as discussed in several previous studies (e.g., Warner et al. 2015).

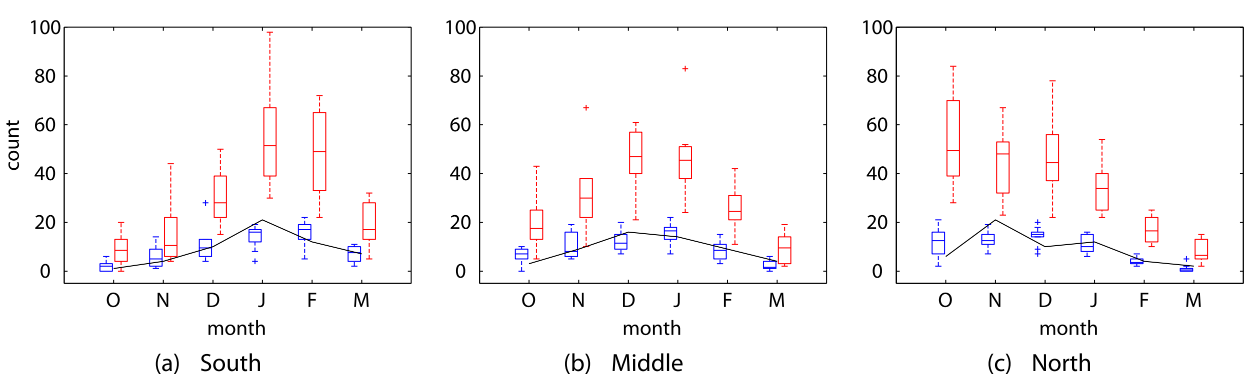

FIG. 4. Box-and-whisker plots of 10-model winter mean (October–March) climatology of AR days defined by 99th percentile IVT offshore at (a) 33.75°, (b) 41.25°, and (c) 47.5°N for the historical (1970–99, blue) and defined by the historical IVT threshold for future periods (2070–99, red). The plots show the median (horizontal lines), the 75th and 25th percentiles (upper and lower range of the box, respectively), the model extremes (whiskers), and outliers from the interquartile range (plus signs). NCEP–NCAR reanalyses events are represented by black solid lines. All locations and months exhibit statistically significant changes in the mean with 95% confidence.

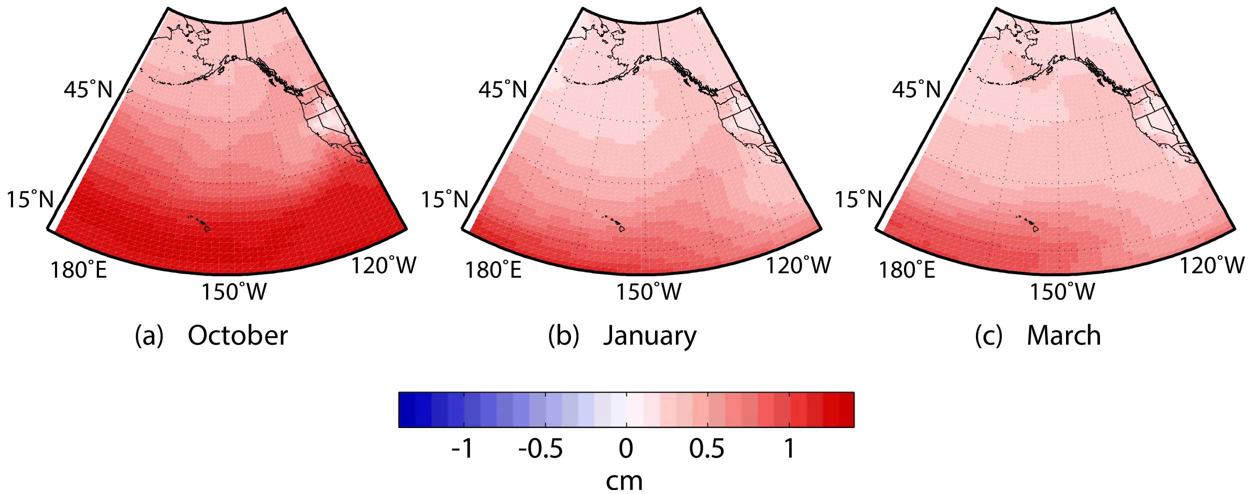

FIG. 5. The 10-model monthly mean IWV (cm) difference between future (2070–99) and historical (1970–99) periods during (a) October, (b) January, and (c) March.

Focusing on the origin of the changes in the historical threshold exceedance, why are the largest projected increases in the frequency of extreme IVT (AR) events found in autumn (and particularly October) to the north, while farther south the biggest increases occur in midwinter? A major contributor to the autumn increases in the north is the large enhancement in climatological IWV (and surface temperature, not shown) over the North Pacific during autumn (e.g., October) in CMIP5 future model projections; in contrast, IWV increases in winter and spring are more modest. These differences are illustrated in Fig. 5, which shows the changes in IWV between historical and end-of-century periods for October, January, and March. October presents substantial increases everywhere, but with particularly large enhancement in the subtropics and tropics; changes in IWV are substantially attenuated in March, particularly in the lower latitudes. Figure 6 shows weak but increasing monthly mean 850-hPa zonal wind along the Washington and Oregon coast early in the season (October) with very little change along the California coast. None of these changes near the coast are statistically significant, consistent with Warner et al. (2015). Throughout the winter and spring, zonal wind values decrease slightly near the Pacific Northwest coast and generally increase along the California coast (opposite from earlier in the season), again, not statistically significant. Thus, with substantial increases in water vapor content over the North Pacific during a season of climatologically strengthening

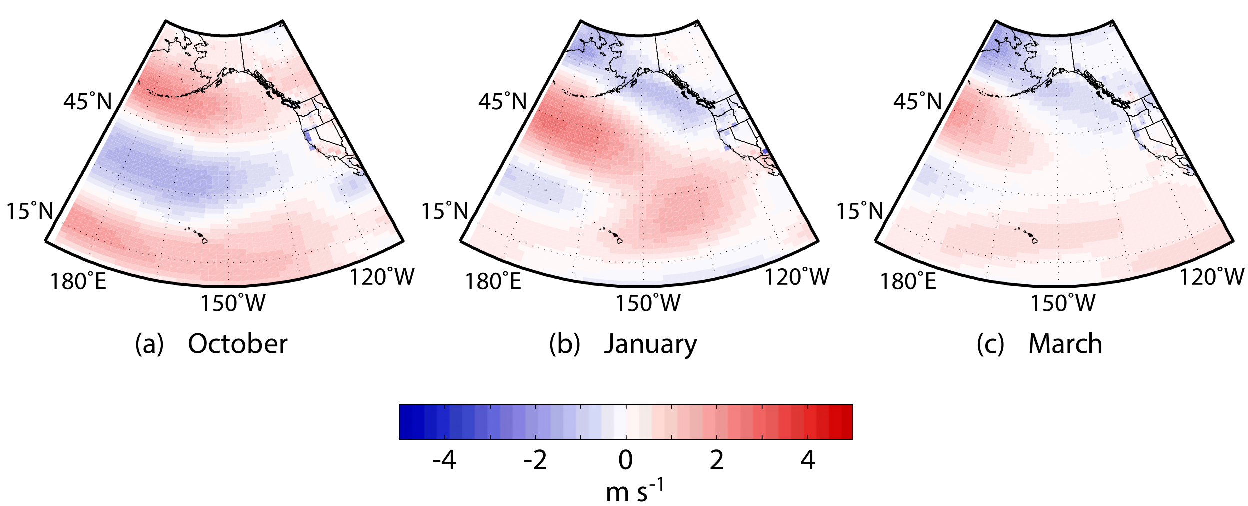

FIG. 6. The 10-model monthly mean 850-hPa u-wind (m s^{-1}) difference between future (2070–99) and historical (1970–99) periods during (a) October, (b) January, and (c) March.

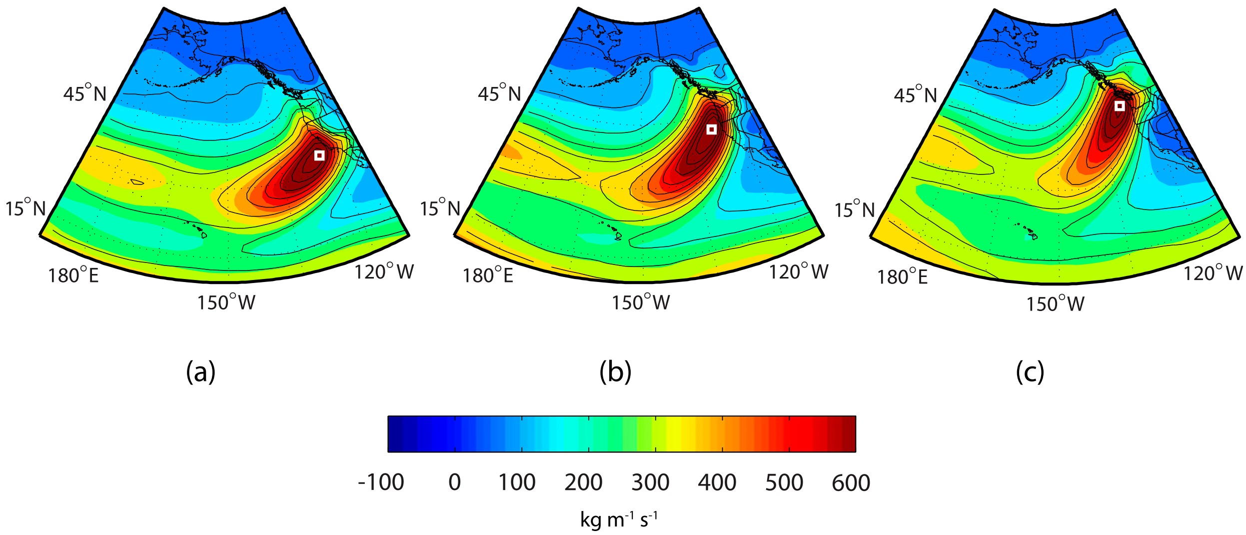

FIG. 7. The 10-model mean 99th percentile average IVT (kg m^{-1} s^{-1}) over the northeast Pacific Ocean for the historical (1970–99, contours) and future periods (2070–99, shading) offshore at (a) 33.75°, (b) 41.25°, and (c) 47.5°N. Historical contours range from 0 to 600 kg m^{-1} s^{-1}.

onshore low-level flow (autumn), the result is substantially enhanced IVT over the northern coast in autumn. In contrast, because of the larger increases in low-level flow near California during the late autumn and winter, the major impacts of increasing IWV are not felt until later in the cool season along the southern portions of the West Coast, even though increases in mean IWV are somewhat attenuated during late winter and spring. The results found here reinforce previous findings of AR changes dominated by increased IWV, with changes in onshore flow playing a secondary role (Warner et al. 2015; Payne and Magnusdottir 2015).

b. AR structure

An important question is whether the structure of moisture plumes associated with atmospheric river events will change under global warming. Figure 7 shows the10-model composite of IVT for the 99th percentile events at three points of the along-coastal transect (33.75°, 41.25°, and 47.5°N) for both the historical (1970–99, contours) and future (2070–99, shading) periods.[5] In each location, the IVT plume extends southwest from the coast toward the Hawaiian Islands. Significantly, the historical and future IVT structures are nearly unchanged, indicating very little alteration in the mean orientations and structures of future ARs impacting the West Coast in a warming world. This, in turn, implies that associated synoptic circulations are also relatively unaltered. Analogous composites at the remaining points show similar results. Since IVT and precipitation are highly correlated during AR events (i.e., Neiman et al. 2002; Ralph et al. 2006; Neiman et al. 2008a; Viale and Nuñez 2011), the IVT structures associated with coastal high precipitation/atmospheric river events are expected to change little under global warming.

Next, examining the variability of the structures among the model projections, Fig. 8 shows the standard deviations of the ensemble-mean IVT for the 99th percentile events for both historical and future periods using the same three points. The structures of the standard deviations are similar for the two time periods, but there are some minor alterations (mainly displacements). In general, the largest variance is to the south of the main IVT plumes, with the variance decreasing for ARs making landfall farther north. At the north point, historical and future variability are nearly collocated, with the suggestion of a second lobe of variability to the north of the IVT plume in both the historical and future means. For the southern and central points, maximum variability appears to be displaced southward for the future projections. The southward displacement of maximum IVT variability for the southern and central points might be explained by the substantially increased water vapor content and increasing late-season low-level winds offshore of central and Southern California at the end of the century (Figs. 5, 6).

To illustrate the variability among the ensemble members, Fig. 9 shows the structure of the historical and

[5] Since spatial structures are being compared for two periods, the 99th percentile method is being used in both periods, instead of the threshold method for the future period, so an equal number of events are composited in each period. This is the case for the remainder of the document.

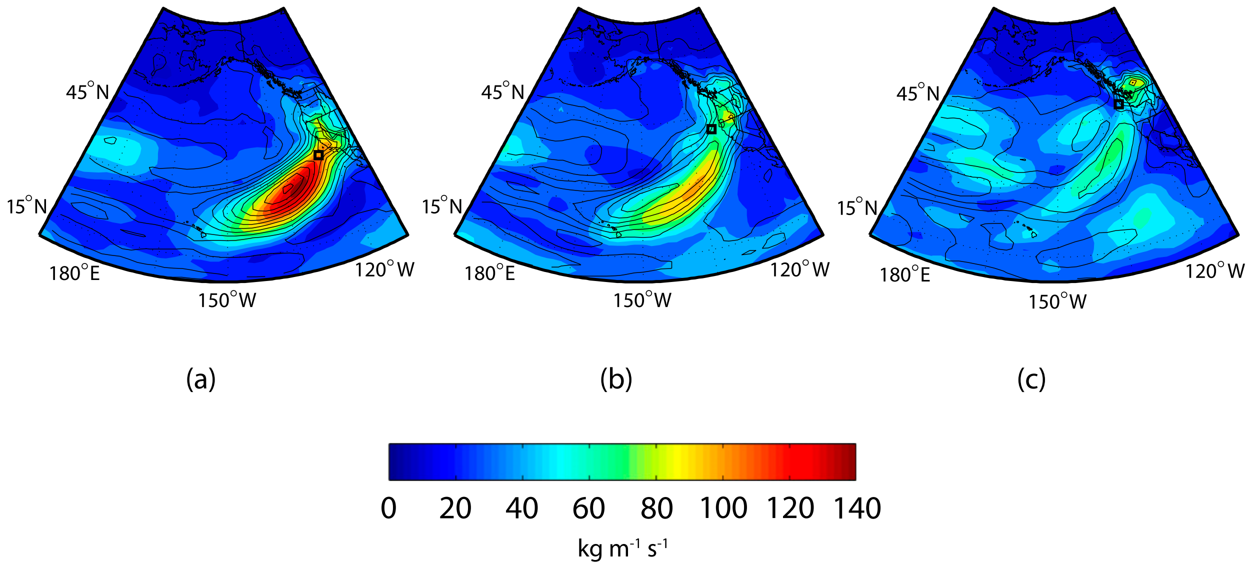

FIG. 8. The 10-model mean 99th percentile std dev of IVT (kg $m^{-1} s^{-1}$) over the northeast Pacific Ocean for the historical (1970–99, contours) and future periods (2070–99, shading) offshore at (a) 33.75°, (b) 41.25°, and (c) 47.5°N. Historical contours range from 0 to 120 kg $m^{-1} s^{-1}$.

future extreme (99th percentile) IVT events for a point near the Oregon–California border for the 10 GCMs used in this study. In general, the structures are similar among the GCMs, with a plume of large IVT stretching southward from the coast. Strikingly, the IVT structures for all models are relatively unchanged between historical and future periods. The intensity changes of the IVT plumes between historical and future periods are generally similar among the models (Fig. 10), with a tendency to intensify the plumes and extend them to the southwest. Together, Figs. 9 and 10 show that the changes from historical to future periods are dominated by intensity change rather than a spatial displacement.

If the structural composites are computed for future events that exceed the historical 99th percentile IVT threshold (rather than the 99th percentile in the future), the composite mean looks very similar to the historical composite (not shown), the only difference being a decrease in the overall IVT plume intensity (since lesser days not previously included are being added to the

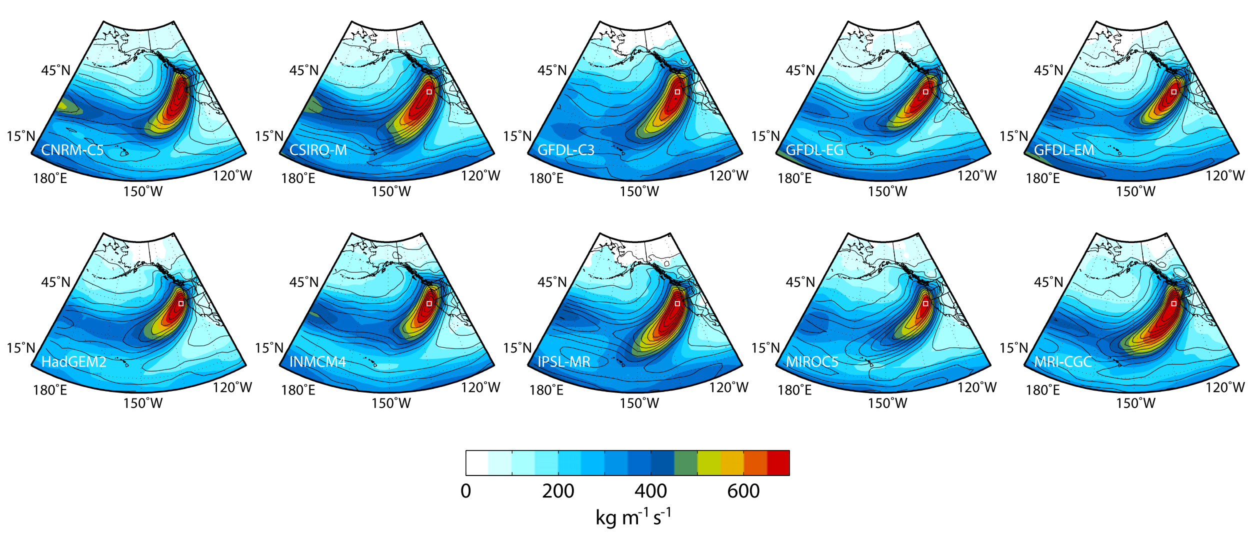

FIG. 9. Mean IVT (kg $m^{-1} s^{-1}$) for 99th percentile days intersecting 41.25°N latitude offshore in each of 10 CMIP5 models. Black contours represent the historical period (1970–99) and color shading represents the future period (2070–99). Historical contours range from 0 to 600 kg $m^{-1} s^{-1}$.

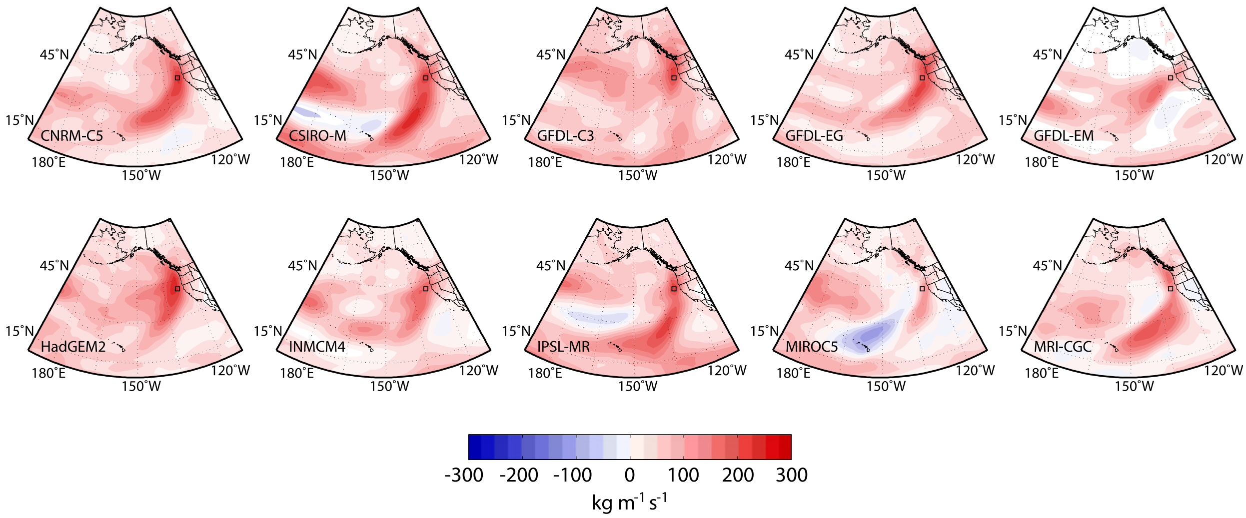

FIG. 10. Difference between future (2070–99) and historical (1970–99) mean IVT (kg m^{-1} s^{-1}) for 99th percentile days intersecting 41.25°N latitude offshore in each of 10 CMIP5 models.

composite). Other variables such as IWV, 500-hPa geopotential height, surface temperature, and u and v winds were also composited for 99th percentile IVT events (not shown). Such composites are very similar to those shown in previous studies based on analyses of observational data (Lackmann and Gyakum 1999; Neiman et al. 2008b; Warner et al. 2012) with only minimal structural differences between historical and future composites. In short, based on CMIP5 simulations, the synoptic-scale IWV/IVT structures associated with atmospheric rivers appear to change minimally with global warming.

4. Discussion and conclusions

This paper describes changes in the climatology, structure, and seasonality of atmospheric rivers influencing the west coast of North America by examining the projections of 10 CMIP5 climate models that used the RCP 8.5 emissions scenario. Specifically, changes in the monthly frequency of extreme atmospheric river events and the accompanying synoptic moisture structures are presented at three locations along the U.S. West Coast. Extreme events are defined as the 99th percentile values of daily averaged IVT at these points during both historical and future time periods. This criterion is different than, but complementary to, approaches applied in many other studies (e.g., Gao et al. 2015; Hagos et al. 2016), which explicitly require the existence of moisture plumes of specific length, magnitude, or width. This paper also examines changes in the seasonality and structure of AR-related moisture plumes, a topic given only modest attention in past studies.

The CMIP5 10-model mean AR composites of high IVT for a historical period (1970–99) are similar to observation-based historical composites presented in previous studies (Lackmann and Gyakum 1999; Neiman et al. 2008b; Warner et al. 2012) and at the three West Coast locations, with a plume of high IVT stretching southwestward from the coast. The NCEP–NCAR reanalyses appear to indicate a peak in extreme IVT roughly one month earlier than the CMIP5 simulations for the historical period, although only southern locations are statistically significant. In general, cool-season extreme IVT events in future projections (2070–99) appear to occur roughly one month earlier than in the historical period, particularly over the southern half of the U.S. West Coast, where some changes are statistically significant. This earlier phasing can be explained by the large increases in IWV during autumn over the northeast Pacific under global warming, with lesser increases during the winter and spring. These IWV changes, in concert with the increased low-level zonal winds over the northern portion of the domain during autumn, may result in an earlier IVT peak in the north. In contrast, the southern maximum is found later in the winter and enhanced by positive changes in low-level winds during that time. These findings are consistent with Dettinger (2011), who found advances in the timing of extreme precipitation events in the future using seven Intergovernmental Panel on Climate Change Fourth Assessment Report climate models at a single location along the Northern California coast. Similarly, Salathé et al. (2014) found increases in future flood risk in the early fall using downscaled regional climate models over the Pacific Northwest.

Considering the number of future days exceeding the historical 99th percentile threshold, there are large, statistically significant increases in extreme IVT events in all months and all locations, with a similar 1–2-month advance in timing. Other studies have also projected large increases in IVT by the end of the century, both globally (i.e., Shields and Kiehl 2016a) and regionally (e.g., Warner et al. 2015). The implication is that society will need to prepare for a substantially more intense precipitation environment by the end of the century (e.g., Allen and Ingram 2002; Pall et al. 2007).

Composites of IVT for extreme (AR) events impacting West Coast points indicate very little structural change in IVT in the future, suggesting that the synoptic flow associated with extreme precipitation events along the West Coast will be relatively unaltered by global warming. This finding is consistent with several studies indicating very small shifts in jet streams and storm tracks over the North Pacific Ocean (i.e., Barnes and Polvani 2013). Individual CMIP5 models also suggest the same: little change in IWV and IVT structures associated with extreme precipitation events along the West Coast by the end of the twenty-first century. These results, and further inspection of the individual CMIP5 projections, do not suggest a significant change in the frequency of ARs approaching the coast from different directions or with differing structures than currently observed, in contrast to the hypothesis of Salathé et al. (2014).

Finally, examination of the structures of historical and projected IVT variance along the West Coast indicates little structure change, but a shift southward along the southern portion of the West Coast, similar to other recent results (Payne and Magnusdottir 2015; Shields and Kiehl 2016a). One contributor is probably the enhancement of IWV that develops southwest of California under future global warming scenarios, but an analysis of this feature is left for future work.

Acknowledgments. This research was supported by the National Science Foundation Grant AGS-1041879 to the second author. The authors thank Dr. Eric Salathé for thoughtful conversations during early stages of this project that contributed greatly to this research. Furthermore, three anonymous reviewers and the JHM editor, Dr. Ruby Leung, provided helpful suggestions and comments.

REFERENCES

Allen, M. R., and W. J. Ingram, 2002: Constraints on future changes in climate and the hydrologic cycle. *Nature*, **419**, 224–232, doi:10.1038/nature01092.

Barnes, E. A., and L. Polvani, 2013: Response of the midlatitude jets, and of their variability, to increased greenhouse gases in the CMIP5 models. *J. Climate*, **26**, 7117–7135, doi:10.1175/JCLI-D-12-00536.1.

Browning, K. A., and C. W. Pardoe, 1973: Structure of low-level jet streams ahead of mid-latitude cold fronts. *Quart. J. Roy. Meteor. Soc.*, **99**, 619–638, doi:10.1002/qj.49709942204.

Chang, E. K. M., Y. Guo, and X. Xia, 2012: CMIP5 multimodel ensemble projection of storm track change under global warming. *J. Geophys. Res.*, **117**, D23118, doi:10.1029/2012JD018578.

Cordeira, J. M., F. M. Ralph, and B. J. Moore, 2013: The dessvelopment and evolution of two atmospheric rivers in proximity to western North Pacific tropical cyclones in October 2010. *Mon. Wea. Rev.*, **141**, 4234–4255, doi:10.1175/MWR-D-13-00019.1.

Dettinger, M., 2004: Fifty-two years of "Pineapple-Express" storms across the west coast of North America. PIER Project Rep. CEC-500-2005-004, California Energy Commission, 20 pp. [Available online at http://www.energy.ca.gov/2005publications/CEC-500-2005-004/CEC-500-2005-004.PDF.]

——, 2011: Climate change, atmospheric rivers, and floods in California—A multimodel analysis of storm frequency and magnitude changes. *J. Amer. Water Resour. Assoc.*, **47**, 514–523, doi:10.1111/j.1752-1688.2011.00546.x.

Gao, Y., J. Lu, L. R. Leung, Q. Yang, S. Hagos, and Y. Qian, 2015: Dynamical and thermodynamical modulations on future changes of landfalling atmospheric rivers over western North America. *Geophys. Res. Lett.*, **42**, 7179–7186, doi:10.1002/2015GL065435.

Hagos, S. M., L. R. Leung, J.-H. Yoon, J. Lu, and Y. Gao, 2016: A projection of changes in landfalling atmospheric river frequency and extreme precipitation over western North America from the large ensemble CESM simulations. *Geophys. Res. Lett.*, **43**, 1357–1363, doi:10.1002/2015GL067392.

Kalnay, E., and Coauthors, 1996: The NCEP/NCAR 40-Year Reanalysis Project. *Bull. Amer. Meteor. Soc.*, **77**, 437–471, doi:10.1175/1520-0477(1996)077<0437:TNYRP>2.0.CO;2.

Lackmann, G. M., and J. R. Gyakum, 1999: Heavy cold-season precipitation in the northwestern United States: Synoptic climatology and an analysis of the flood of 18 January 1986. *Wea. Forecasting*, **14**, 687–700, doi:10.1175/1520-0434(1999)014<0687:HCSPIT>2.0.CO;2.

Lavers, D. A., R. P. Allan, G. Villarini, B. Lloyd-Hughes, D. J. Brayshaw, and A. J. Wade, 2013: Future changes in atmospheric rivers and their implications for winter flooding in Britain. *Environ. Res. Lett.*, **8**, 034010, doi:10.1088/1748-9326/8/3/034010.

——, F. M. Ralph, D. E. Waliser, A. Gershunov, and M. D. Dettinger, 2015: Climate change intensification of horizontal water vapor transport in CMIP5. *Geophys. Res. Lett.*, **42**, 5617–5625, doi:10.1002/2015GL064672.

Lu, J., G. A. Vecchi, and T. Reichler, 2007: Expansion of the Hadley cell under global warming. *Geophys. Res. Lett.*, **34**, L06805, doi:10.1029/2006GL028443.

Mass, C., A. Skalenakis, and M. Warner, 2011: Extreme precipitation over the west coast of North America: Is there a trend? *J. Hydrometeor.*, **12**, 310–318, doi:10.1175/2010JHM1341.1.

Mastin, M. C., A. S. Grendaszek, and C. R. Barnas, 2010: Magnitude and extent of flooding at selected river reaches in western Washington, January 2009. USGS Scientific Investigations Rep. 2010-5177, 34 pp. [Available online at https://pubs.usgs.gov/sir/2010/5177/pdf/sir20105177.pdf.]

Meehl, G., and Coauthors, 2007: Global climate projections. *Climate Change 2007: The Physical Science Basis*, S. Solomon et al., Eds., Cambridge University Press, 747–845.

Mundhenk, B. D., E. A. Barnes, and E. D. Maloney, 2016: All-season climatology and variability of atmospheric river frequencies over the North Pacific. *J. Climate*, **29**, 4885–4903, doi:10.1175/JCLI-D-15-0655.1.

Neiman, P. J., F. M. Ralph, A. B. White, D. E. Kingsmill, and P. O. G. Persson, 2002: The statistical relationship between upslope flow and rainfall in California's coastal mountains: Observations during CALJET. *Mon. Wea. Rev.*, **130**, 1468–1492, doi:10.1175/1520-0493(2002)130<1468:TSRBUF>2.0.CO;2.

——, ——, G. A. Wick, Y.-H. Kuo, T.-K. Wee, Z. Ma, G. H. Taylor, and M. D. Dettinger, 2008a: Diagnosis of an intense atmospheric river impacting the Pacific Northwest: Storm summary and offshore vertical structure observed with COSMIC satellite retrievals. *Mon. Wea. Rev.*, **136**, 4398–4420, doi:10.1175/2008MWR2550.1.

——, ——, ——, J. D. Lundquist, and M. D. Dettinger, 2008b: Meteorological characteristics and overland precipitation impacts of atmospheric rivers affecting the west coast of North America based on eight years of SSM/I satellite observations. *J. Hydrometeor.*, **9**, 22–47, doi:10.1175/2007JHM855.1.

——, L. J. Schick, F. M. Ralph, M. Hughes, and G. A. Wick, 2011: Flooding in western Washington: The connection to atmospheric rivers. *J. Hydrometeor.*, **12**, 1337–1358, doi:10.1175/2011JHM1358.1.

Pall, P., M. Allen, and D. Stone, 2007: Testing the Clausius–Clapeyron constraint on changes in extreme precipitation under CO_2 warming. *Climate Dyn.*, **28**, 351–363, doi:10.1007/s00382-006-0180-2.

Payne, A. E., and G. Magnusdottir, 2015: An evaluation of atmospheric rivers over the North Pacific in CMIP5 and their response to warming under RCP 8.5. *J. Geophys. Res. Atmos.*, **120**, 11 173–11 190, doi:10.1002/2015JD023586.

Ralph, F. M., P. J. Neiman, and R. Rotunno, 2005: Dropsonde observations in low-level jets over the northeastern Pacific Ocean from CALJET-1998 and PACJET-2001: Mean vertical-profile and atmospheric-river characteristics. *Mon. Wea. Rev.*, **133**, 889–910, doi:10.1175/MWR2896.1.

——, ——, G. A. Wick, S. I. Gutman, M. D. Dettinger, D. R. Cayan, and A. B. White, 2006: Flooding on California's Russian River: Role of atmospheric rivers. *Geophys. Res. Lett.*, **33**, L13801, doi:10.1029/2006GL026689.

——, T. Coleman, P. J. Neiman, R. J. Zamora, and M. D. Dettinger, 2013: Observed impacts of duration and seasonality of atmospheric-river landfalls on soil moisture and runoff in coastal Northern California. *J. Hydrometeor.*, **14**, 443–459, doi:10.1175/JHM-D-12-076.1.

Rutz, J. J., W. J. Steenburgh, and F. M. Ralph, 2014: Climatological characteristics of atmospheric rivers and their inland penetration over the western United States. *Mon. Wea. Rev.*, **142**, 905–921, doi:10.1175/MWR-D-13-00168.1.

Ryoo, J.-M., D. E. Waliser, D. W. Waugh, S. Wong, E. J. Fetzer, and I. Fung, 2015: Classification of atmospheric river events on the US West Coast using a trajectory model. *J. Geophys. Res. Atmos.*, **120**, 3007–3028, doi:10.1002/2014JD022023.

Salathé, E. P., Jr., 2006: Influences of a shift in North Pacific storm tracks on western North American precipitation under global warming. *Geophys. Res. Lett.*, **33**, L19820, doi:10.1029/2006GL026882.

——, A. F. Hamlet, C. F. Mass, S. Lee, M. Stumbaugh, and R. Steed, 2014: Estimates of twenty-first-century flood risk in the Pacific Northwest based on regional climate model simulations. *J. Hydrometeor.*, **15**, 1881–1899, doi:10.1175/JHM-D-13-0137.1.

Shields, C. A., and J. T. Kiehl, 2016a: Atmospheric river landfall-latitude changes in future climate simulations. *Geophys. Res. Lett.*, **43**, 8775–8782, doi:10.1002/2016GL070470.

——, and ——, 2016b: Simulating the Pineapple Express in the half-degree Community Climate System Model, CCSM4. *Geophys. Res. Lett.*, **43**, 7767–7773, doi:10.1002/2016GL069476.

Singh, M. S., and P. A. O'Gorman, 2012: Upward shift of the atmospheric general circulation under global warming: Theory and simulations. *J. Climate*, **25**, 8259–8276, doi:10.1175/JCLI-D-11-00699.1.

Sodemann, H., and A. Stohl, 2013: Moisture origin and meridional transport in atmospheric rivers and their association with multiple cyclones. *Mon. Wea. Rev.*, **141**, 2850–2868, doi:10.1175/MWR-D-12-00256.1.

Viale, M., and M. N. Nuñez, 2011: Climatology of winter orographic precipitation over the subtropical central Andes and associated synoptic and regional characteristics. *J. Hydrometeor.*, **12**, 481–507, doi:10.1175/2010JHM1284.1.

Warner, M. D., C. F. Mass, and E. P. Salathé, 2012: Wintertime extreme precipitation events along the Pacific Northwest coast: Climatology and synoptic evolution. *Mon. Wea. Rev.*, **140**, 2021–2043, doi:10.1175/MWR-D-11-00197.1.

——, ——, and ——, 2015: Changes in winter atmospheric rivers along the North American West Coast in CMIP5 climate models. *J. Hydrometeor.*, **16**, 118–128, doi:10.1175/JHM-D-14-0080.1.